Accelerated Expansion of Laser-Ablated Materials near a Solid Surface

K. R. Chen,* J. N. Leboeuf, R. F. Wood, D. B. Geohegan, J. M. Donato, C. L. Liu, and A. A. Puretzky
Oak Ridge National Laboratory, Oak Ridge, Tennessee 37831-8071
(Received 22 August 1995)

A dynamic source effect that accelerates the expansion of laser-ablated material in the direction perpendicular to the target is demonstrated. A self-similar theory shows that the maximum expansion velocity is proportional to c_s/α, where $1 - \alpha$ is the slope of the velocity profile and c_s is the sound speed. Numerical hydrodynamic modeling is in good agreement with the theory. A dynamic partial ionization effect is also studied. With these effects, α is reduced and the maximum expansion velocity is significantly increased over that found from conventional models.

PACS numbers: 79.20.Ds, 03.40.Gc, 47.45.–n, 81.15.Fg

The behavior of material expanding into a vacuum or ambient background is an important issue in gas dynamics [1–6]. It is of interest in materials research [7–18], fluid dynamics [2], chemical physics [4,13], plasma sciences [4–6], detonation processes [4–6,19], cosmology [3,4,20], and many other disciplines. It has long been an important conclusion [1–5,13] that the escape (maximum expansion or expansion front) velocity of an originally stationary gas has a limit, which for an ideal gas is $c_s\sqrt{2/(\gamma - 1)}$ for a steady expansion and $2c_s/(\gamma - 1)$ for an unsteady expansion, where c_s is the initial sound speed and γ is the ratio of specific heats.

For laser ablation in materials research, the quality of the deposited films is critically dependent on the range and profile of the kinetic energy and density of the ablated plume [7–9]. Experimental measurements consistently show that, at low laser fluence for which the laser energy absorbed by the plume is thought to be negligible, the expansion front is a factor of 2–3 faster than predicted from unsteady adiabatic expansion with typical vaporization temperatures [7,10–13]. The effect of a Knudsen layer [15] was studied in an attempt to explain the higher escape velocity. It gives a velocity of $4u_k$ [13], where $u_k < c_s$ is the Knudsen layer velocity, which is still too low. The inability to explain the experimental observation through gas dynamics has prompted a suggestion [14] of increased vapor temperature due to violent interactions inside the target such as "phase explosion" [17].

In this Letter we demonstrate for the first time a dynamic source effect that accelerates the unsteady expansion front in the direction perpendicular to the target surface significantly faster than predicted from conventional models. The related effect of dynamic partial ionization that increases the expansion in all directions is also studied. These results may help explain the long-time puzzle of high expansion front velocities observed in laser-ablation experiments without introducing more exotic mechanisms. As in previous work [11–14], we are interested here in a laser fluence range high enough for hydrodynamic theory to be applicable but low enough for the absorption of the laser energy by the plume to be weak so that we can compare with free expansion models that do not include absorption.

In free expansion models the material that will form the plume is initially held in a reservoir. At $t = 0$, when the gate of the reservoir at $x = 0$ is opened, the gas adiabatically expands forward and a rarefaction wave moves with the sound speed from the gate to the back wall at $x = -d$ in a period of time (t_r) during which the back wall pressure remains constant. Then, the wall pressure begins to drop quickly. For the expansion remaining self-similar $(t \le t_r)$, the average velocity gained per particle involved in the expansion is c_s/γ. For monatomic gases $\gamma = \frac{5}{3}$, the maximum velocity is $3c_s$ and the velocity and density profiles of the expanding gas are $v = 3c_s(1/4 + x/4c_st)$ and $n = n_0(3/4 - x/4c_st)^3$, respectively [1–5,13], where $c_s = (\gamma k_B T_v/m)^{1/2}$, k_B is the Boltzmann constant, T_v is the vapor temperature, m is the mass of the plume atoms, and n_0 is the initial gas density.

In our approach, chosen to correspond more accurately to the true physical situation, the material with the same temperature is inserted as a source dynamically introduced into the system at $x = 0$ after $t = 0$. For the plume pressure P below its thermodynamic critical pressure and with low plume viscosity, we may assume that the plume behaves as an ideal gas such that $P = n(1 + \eta)k_BT$, where n (T) is the density (temperature) of the plume, and η is the ionization fraction. We use Euler's equations to model the plume dynamics and the Saha equation to determine the ionization fraction [16]:

$$\frac{\partial}{\partial t}(n) = -\frac{\partial}{\partial x}(nv) + S_n\delta(x - x_s), \tag{1}$$

$$m\frac{\partial}{\partial t}(nv) = -\frac{\partial}{\partial x}(P + mnv^2), \tag{2}$$

$$\frac{\partial}{\partial t}(E) = -\frac{\partial}{\partial x}[v(E + P)] + S_E\delta(x - x_s), \tag{3}$$

$$\frac{\eta^2}{1 - \eta} = \frac{2}{n}\frac{u_+}{u_0}\left(\frac{2\pi m_e k_B T}{h^2}\right)^{3/2} e^{-U_i/k_BT}, \tag{4}$$

where $E = mne + mnv^2/2$ is the energy density, $e = (1 + \eta)(k_BT/m)/(\gamma - 1) + \eta U_i$ is the enthalpy,

 0031-9007/95/75(25)/4706(4)$06.00

U_i is the ionization energy, u_+ and u_0 are the electronic partition functions, m_e is the electron mass, h is Planck's constant, $S_n = n_{\rm liq} v_{\rm rs}$ is the density source, $S_E = n_{\rm liq} v_{\rm rs} k_B T_v/(\gamma - 1)$ is the energy source, $n_{\rm liq}$ is the liquid density, and $v_{\rm rs}$ is the recession speed of the target surface due to ablation. Here we take the small Knudsen layer limit, use $v = 0$ at the surface, and let S_n and S_E be constant. Because $c_s \gg v_{\rm rs}$, the effect of surface recession on the plume expansion can be neglected [21], i.e., $x_s = 0$.

Intuitive physical explanation.—For the system without any ablated material at $t = 0$, we expect that at $t > 0$ the surface pressure rises due to the dynamic source and the gas expansion decreases the rise rate. Then, the balance between them causes the surface pressure to saturate. Since the plume momentum is determined by the pressure gradient, the sustained pressure may yield higher average velocities at early times. Moreover, the accompanying source of energy inflow also makes the unsteady expansion nonadiabatic, especially near the surface. During an unsteady expansion, the kinetic energy of the plume is redistributed. The increase of entropy due to nonadiabaticity further changes the plume profiles and may thus result in an even higher maximum expansion velocity, especially in the direction perpendicular to the surface. This will be studied analytically.

The effect of dynamic partial ionization further increases the maximum expansion velocity, but in all directions. When the material expands into a background gas, a shock wave is generated at the expansion front. As a result, the temperature at the front increases. With dynamic partial ionization some of the heat is transferred to ionization energy such that the increase of the temperature at the front becomes smaller to balance the plume enthalpy. That is, less energy goes to thermal (or random) motion. Simultaneous conservation of energy and momentum causes the flow velocity to become larger, which represents directed motion. This effect is reduced for lower vapor temperature. It has no effect when the material is fully ionized. We will quantify the effect with numerical modeling.

A self-similar theory for the dynamic source effect.—For simplicity and comparison with the free expansion results, our analysis considers the gas expanding into a vacuum to be neutral, which is a good approximation for $T_v \ll U_i$. With an energy source, the system is not adiabatic near the surface. Nevertheless, except for early times and a transition region (δx) near the surface, we expect self-similar expansion as in a free expansion. The self-similar variable is $\xi \equiv x/v_m t$, where v_m is the maximum expansion velocity, and the velocity profile is $v = v_m[\alpha + (1 - \alpha)\xi]$, where α is determined by the flow properties ($1 \geq \alpha \geq 0$) and is expected to be different from that of adiabatic free expansion, i.e., $\alpha = (\gamma - 1)/(\gamma + 1)$. The source boundary conditions at $\xi = \delta \equiv \delta x/v_m t \ll 1$ are given by the constants $n = n_\delta$, $T = T_\delta$, and $v = v_\delta$. We transform the independent variables from (x, t) to ξ. From Eqs. (1) and (2) we obtain the density profile $n = n_\delta(1 - \xi)^{(1-\alpha)/\alpha}$ and the pressure profile $P = n_\delta \times v_m^2 m \alpha^2 (1 - \alpha)/(1 + \alpha)(1 - \xi)^{(1+1/\alpha)}$. The temperature profile is then $k_B T/m = v_m^2 \alpha^2 (1 - \alpha)/(1 + \alpha)(1 - \xi)^2$.

Thus, the plume profiles are known, except for v_m, α, n_δ, and T_δ. From mass conservation, we have

$$v_m = n_{\rm liq} v_{\rm rs}/n_\delta \alpha\,, \tag{5}$$

which shows that the mass flux at δ equals the mass source. When P_δ is approximated to be a constant in time, the conservation of momentum gives

$$v_m = c_\delta/\alpha\sqrt{\gamma g}\,, \tag{6}$$

where $g = (1 - \alpha)/(1 + \alpha)$ and $c_\delta = (\gamma k_B T_\delta/m)^{1/2}$. The energy conservation yields

$$v_m = c_s/\alpha\sqrt{\gamma h}\,, \tag{7}$$

where $h = [2(1 - \alpha) + (5 + \alpha)(\gamma - 1)]/2(1 + \alpha) \times (1 + 2\alpha)$. So far, we have three equations for four unknowns. We need one more equation to uniquely determine the solution. This requires the solution of the nonlinear equations in the transition region near the surface, where the entropy increases. Instead of introducing this complexity, numerical hydrodynamic modeling is used. From the slope of the velocity profile found from this modeling, a value of α is obtained, which then allow us to compare other parameters and profiles with the analytical solutions. We note that if $\alpha = (\gamma - 1)/(\gamma + 1)$ is used, the analytical theory can recover the previous results [13] of free expansion with a Knudsen layer.

The analytic results show interesting physics. From the plume profiles, we know that the lower the constant α, the more nonuniform the flow. Also, Eqs. (5)–(7) indicate that lower α implies higher v_m. Figure 1 shows v_m, normalized to c_s and c_δ, as a function of α for a monatomic gas $\gamma = \frac{5}{3}$. The rapid rise of the maximum expansion velocity at $\alpha \leq 0.1$ is due to the $1/\alpha$ dependence. The value $v_m/c_\delta = 4$ for $\alpha = \frac{1}{4}$ corresponds to the case of adiabatic expansion with a Knudsen layer [13]. Equation (6) gives the local flow condition at δ, i.e., $v_\delta/c_\delta = \sqrt{(1 + \alpha)/\gamma(1 - \alpha)}$. The flow at δ is sonic for the case of adiabatic expansion with the Knudsen layer. Figure 1 also shows that the flow at $\xi = \delta$ is subsonic (supersonic) for $\alpha < \frac{1}{4}$ ($\alpha > \frac{1}{4}$). The local temperature in terms of T_v is not sensitive to α.

Numerical hydrodynamic simulation.—The Rusanov scheme [22] was used to solve Euler's equations, Eqs. (1)–(3); the nonlinear calculation of T and η was done with the Newton-Raphson method [23]. The logarithm of Eq. (4) was used for numerical stability. The system size was 1000 spatial cells, Δx. The initial adaptive grid size was 10^{-5} cm, which is required for numerical convergence. New vapor was added into the first cell near the surface perturbatively; this limited the time step size to $n_{\rm liq} v_{\rm rs} T_v \Delta t \ll n_1 T_1 \Delta x$, with subscript 1 the first cell.

Typical physical parameters were as follows. The system was initialized with a uniform background gas

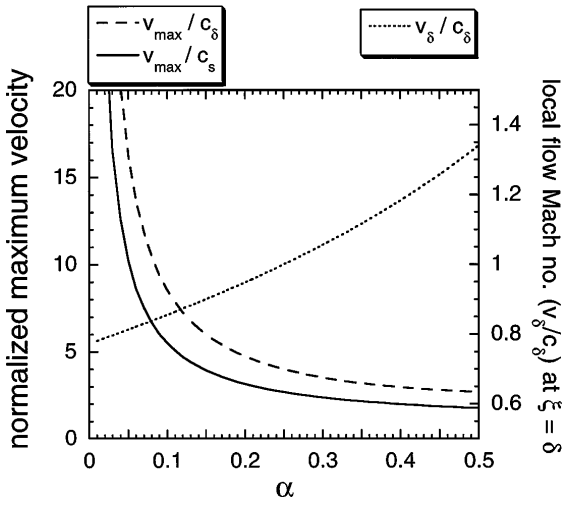

FIG. 1. Normalized maximum expansion velocity and local flow Mach number (v_δ/c_δ) at $\xi = \delta$ as functions of α for $\gamma = \frac{5}{3}$ from self-similar theory. In free expansion models, $\alpha = 0.25$.

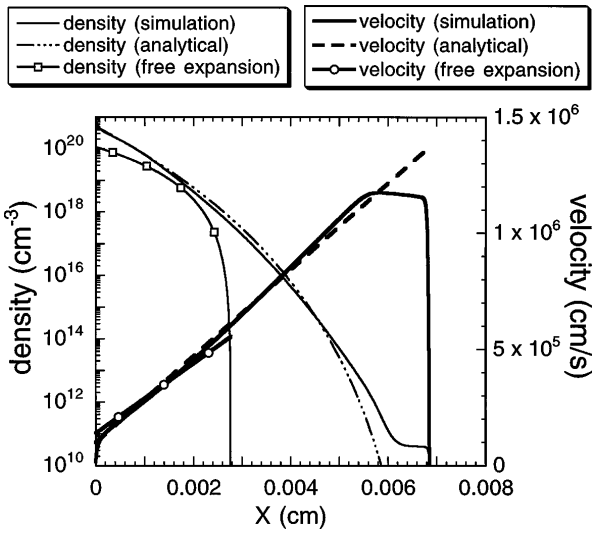

FIG. 2. The plume density and velocity profiles at $t = 5$ ns from the analytical self-similar theory, numerical hydrodynamic modeling, and conventional free expansion model. Here, we have $\alpha = 1/14$ and $v_m = 7.42c_s$ for the analytics, and $n_0 = n_{\rm liq}v_{\rm rs}/c_s = 2.69 \times 10^{20}$ cm^{-3} for the free expansion case.

of density $n_{\rm bg} = 1 \times 10^{10}$ cm^{-3} and temperature $T_{\rm bg} = 293$ K, for a pressure $P_{\rm bg} \sim 0.3$ μTorr. A constant supply of vapor was added for 6 ns with a temperature $T_v = 7000$ K, given by the Clausius-Clapeyron equation for a surface pressure at several hundred atmospheres. The target surface recession speed was $v_{\rm rs} = 1 \times 10^3$ cm/s. These parameters are typical for the ablation of silicon at a laser fluence of a few J/cm^2 [24]. Both source and background gases are chosen to have a mass of 28 amu with a solid density of 5.01×10^{22} cm^{-3}, an ionization potential of 1.3×10^{11} ergs (8.1 eV), $u_+ = 6$, and $u_0 = 15$; these parameters correspond to silicon. The normalized results should also be applicable to different materials. We used $\gamma = \frac{5}{3}$. Thus, $c_s = 1.85 \times 10^5$ cm/s.

We first study the case without the Saha equation (no ionization, i.e., $\eta = 0$). Figure 2 shows the profiles of density and velocity at $t = 5$ ns, at which time the expansion is almost steady state. From the modeling, we found that the expansion developed self-similarly after 0.1 ns. The front position is at $x = 0.0069$ cm at $t = 5$ ns. From the ratio of the front position and the time, we estimate $v_m = 1.38 \times 10^6$ cm/s or $7.46c_s$, which is 2.5 times that predicted from the free expansion model (i.e., $3c_s = 5.55 \times 10^5$ cm/s). From the slope of the velocity profile, we know $\alpha = 1/14 = 0.07143$, which gives $v_\delta = 9.85 \times 10^4$ cm/s. Thus, $\delta x = 6.4 \times 10^{-5}$ cm. The simulation also shows that $n_\delta = 4.7 \times 10^{20}$ cm^{-3} and $T_\delta = 3693$ K. From Eq. (7), the analytical maximum expansion velocity is $7.42c_s$. From Eqs. (5) and (6), $n_\delta = 5.07 \times 10^{20}$ cm^{-3} and $T_\delta = 2836$ K. The analytical profiles, from the self-similar theory, shown in the figure are $n = n_\delta[1 - x/(0.0069\ \text{cm})]^{13}$ and $v = v_m/14 + (13/14)[x/(5\ \text{ns})]$. Although the profiles at the shock front are flattened due to the small but finite background pressure (not included in the analytical theory), the overall profiles and scalings are in good agreement with the analytical theory. The average velocity at 5 ns is 1.8×10^5 cm/s, which is about 60% higher than that of the free expansion model. After the rarefaction wave of the free expansion reaches the back wall, the difference will be significantly reduced (and disappear at $t \to \infty$ if the system remains one dimensional). However, the maximum expansion velocity and the self-similar profile have been reached much earlier. In Fig. 2, for the free expansion case, $n_0 = n_{\rm liq}v_{\rm rs}/c_s$ is chosen to make the total number of atoms involved (and energy) equal to that of the dynamic source case. We note that the pressure in the reservoir is 258 atm, which is smaller than that from the dynamic source case as shown in Fig. 3.

Figure 3 shows how the dynamic source causes the surface pressure to rise quickly and approach a saturation level of 4.7×10^8 dyn/cm^2, or 460 atm, consistent with measured values [18]. Then the surface pressure drops exponentially after the source is terminated at $t = 6$ ns. Maximum velocity at $t = 10$ ns is 1.2×10^6 cm/s.

When we use the Saha equation (the more physical case), we find that the surface pressure remains unchanged and the maximum velocity is about 40% higher as also shown in Fig. 3. It reaches 1.7×10^6 cm/s or $9.2c_s$ at $t = 10$ ns. As discussed earlier, this is an effect due to dynamic partial ionization as a result of increased energy channeled into directed motion. This effect is reduced when the vapor temperature is lower; it gives only about a 6% increase when $T_v = 3500$ K, for example.

When the background pressure is lower, the simulation results show that α is lower, the maximum velocity is higher (which is linear in the log$P_{\rm bg}$ scale), and the effect of dynamic partial ionization is greater. We also checked the effect of different surface recession speeds. Both surface pressure and density are linearly proportional

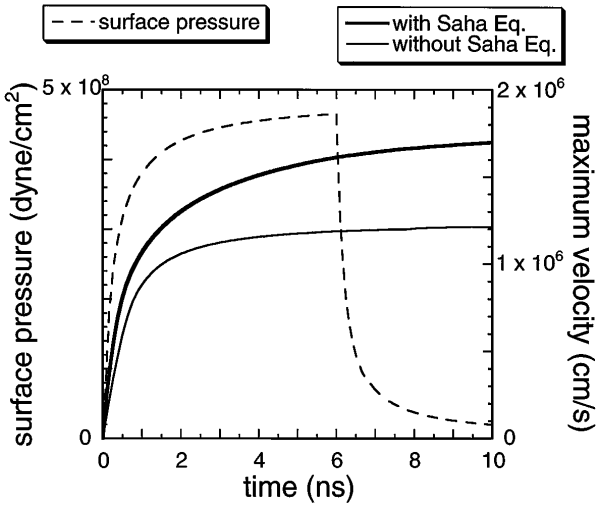

FIG. 3. The histories of the surface pressure and the maximum velocity with and without the Saha equation for ionization. The surface pressure is calculated from a three-point average at the surface. The maximum expansion velocity from the free expansion model is 5.55×10^5 cm/s.

to v_{rs}; thus, the maximum velocity and the profiles are insensitive to it. For low background density, the maximum velocity can be 10 times higher than the source sound speed; that is, the kinetic energy of the front can be 1 order of magnitude higher than that predicted by conventional models. This is consistent with a recent experimental result [10] that the velocity of the expansion front is 1 order of magnitude higher than that of the neutral Si density peak, which can be predicted with typical vaporization temperature. We also note that, when the velocity of the main body of the plume is at the right kinetic energy range for film deposition, the extremely higher kinetic energy of the front may cause film damage.

We have treated the laser-ablated material as a dynamic source, which is closer to experimental conditions than is the constant source used in free expansion models. It is demonstrated that the dynamic source and partial ionization effects can dramatically increase the front expansion velocity, which becomes significantly higher than those predicted from conventional free expansion models, while the average momentum in the direction perpendicular to the solid surface is moderately increased ($\leq 60\%$) at early times. Since the expansion is accelerated mainly in the perpendicular direction, it should become more nonsymmetric and forward peaked. Two-dimensional modeling would be required to study the resultant plume profile and dynamics away from the target surface. The profiles and scalings from numerical hydrodynamic modeling are in good agreement with our self-similar theory. The results may provide an explanation for experimental observations of high expansion front velocities even at low laser fluence without involving more exotic mechanisms. Although this study is applied to laser ablation, it should be of interest in many other scientific disciplines in which ultrarapid gas dynamics are of fundamental importance.

K. R. C. appreciates discussions with J. W. Cobb. This work is supported by the ORNL LDRD Funds, and U.S. DOE under Contract No. DE-AC05-84OR21400. K. R. C. and C. L. L. were supported in part by appointments to the ORNL Research Associate Program administered jointly by ORISE and ORNL.

*Present address: Physics Department, Changhua University of Education, Changhua, Taiwan, Republic of China.

[1] R. Courant and K. O. Friedrichs, *Supersonic Flow and Shock Waves* (Interscience Publishers, New York, 1948).
[2] L. D. Landau and E. M. Lifshitz, *Fluid Mechanics* (Addison-Wesley, New York, 1959), p. 357.
[3] S. A. Kaplan, *Interstellar Gas Dynamics* (Pergamon Press, London, 1966), p. 86.
[4] Ya. B. Zel'dovich and Yu. P. Raizer, *Physics of Shock Waves and High-Temperature Hydrodynamic Phenomena* (Academic Press, New York, 1966).
[5] M. A. Liberman and A. L. Velikovich, *Physics of Shock Waves in Gases and Plasmas* (Springer-Verlag, Berlin, 1986).
[6] Yu. I. Koptev, *Gas Dynamics* (Nova Science Publishers, New York, 1992).
[7] J. F. Ready, *Effects of High-Power Laser Radiation* (Academic Press, Orlando, 1971), pp. 201, 206.
[8] *Pulsed Laser Deposition of Thin Films*, edited by D. B. Chrisey and G. K. Hubler (Wiley & Sons, New York, 1994).
[9] R. K. Singh, O. W. Holland, and J. Narayan, J. Appl. Phys. **68**, 233 (1990).
[10] D. G. Goodwin *et al.*, in *Proceedings of the Symposium on Energy Beams, San Francisco, 1995*, edited by H. A. Atwater *et al.* (MRS, Pittsburgh, 1995).
[11] R. Kelly and R. W. Dreyfus, Surf. Sci. **198**, 263 (1988).
[12] R. Kelly and R. W. Dreyfus, Nucl. Instrum. Methods Phys. Res. Sect. B **32**, 341 (1988).
[13] R. Kelly, J. Chem. Phys. **92**, 5047 (1990).
[14] R. Kelly *et al.* (to be published); R. Kelly (private communication).
[15] C. J. Knight, AIAA J. **17**, 519 (1979).
[16] See, e.g., A. Vertes, in *2nd International Conference on Laser Ablation: Mechanisms and Application—II*, edited by J. C. Miller and D. B. Geohegan, AIP Conf. Proc. No. 288 (AIP, New York, 1993).
[17] M. M. Martynyuk, Sov. Phys. Tech. Phys. **21**, 430 (1976).
[18] P. E. Dyer *et al.*, in *Laser Ablation of Electronic Materials*, edited by E. Fogarassy and S. Lazare (North-Holland, Amsterdam, 1992).
[19] Ch. Sack and H. Schamel, Phys. Rep. **156**, 311 (1987).
[20] M. D. Smith *et al.*, Nature (London) **293**, 277 (1981).
[21] G. Weyl, A. Pirri, and R. Root, AIAA J. **19**, 460 (1981).
[22] G. A. Sod, J. of Comput. Phys. **27**, 1–31 (1978).
[23] W. H. Press *et al.*, *Numerical Recipes (FORTRAN Version)* (1989), p. 267.
[24] From a laser-target model developed from Laser 8, R. F. Wood and G. A. Geist, Phys. Rev. Lett. **57**, 873 (1986).